Eur. Phys. J. E **21**, 223–230 (2006)
DOI 10.1140/epje/i2006-10062-8

THE EUROPEAN PHYSICAL JOURNAL E

Correlation in a Gaussian chain with the ends fixed

K. Kawai and K. Okumura[a]

Department of physics, Graduate School of Humanities and Sciences, Ochanomizu University, Otsuka 2-1-1, Bunkyo-ku, Tokyo 112-8610, Japan

Received 30 August 2006
Published online: 4 January 2007 –

Abstract. We consider an ideal chain whose ends are fixed without fluctuation at different points, possibly by optical tweezers. We derive a two-point probability distribution of a corresponding random walk and explicitly calculate the scattering function. We find that the contour plot of the resulting function shows a kind of normal butterfly pattern, contaminated by wavy texture. These results are compared with some representative previous models.

PACS. 82.35.Lr Physical properties of polymers – 82.37.Rs Single molecule manipulation of proteins and other biological molecules – 05.40.Fb Random walks and Levy flights

1 Introduction

There have been many studies on the correlation in a polymer chain with constraints since the '70s, largely due to the development of the neutron scattering technique on labeled species. For example, they have studied experimentally a polymer elongated in stretched bulk [1] or film [2], or in a shear flow [3], and a polymer chain extended in macroscopically deformed rubber [4] or gel [5]. Here, we discuss the correlation in a polymer chain whose ends are fixed *without fluctuation*; such a situation could be realized and observed in the near future, possibly by well-developed techniques on optical tweezing and single molecular observation [6].

Early works on correlation or scattering function of a chain with external constraints are mainly considered in the context of a chain in networks. Benoit *et al.* considered a chain which deforms affinely [7], and non-affine cases are treated by Pearson [8], which is generalized by Warner and Edwards [9]. In addition to these works for ideal chains, a scaling theory for a stretched self-avoiding chain was constructed [10,11]. Later, for example, theories for the so-called abnormal butterfly pattern of the structure factor observed for stretched swollen gels were developed [12,13].

However, a fundamental situation where an ideal chain is fixed without fluctuation at both ends, which includes the actively studied ring polymers [14–17] as a special case, has not been discussed thoroughly [18,19], although it might be possible in principle to realize such a situation. Here, we derive the probability necessary for the calculation of a pair correlation function of a Gaussian chain with the ends fixed to R without fluctuation, and explicitly calculate the scattering function. The results are compared with previous results developed in the context of a chain in networks. We discuss their possible connections to the scattering from slide-ring gel, which is a new type of gel whose cross-links are neither a chemical nor physical link but a link made by connecting two rings where through each ring one chain passes and each ring is slidable along the chain [20].

[a] e-mail: okumura@phys.ocha.ac.jp (corresponding author)

2 Probability distribution

2.1 Heuristic derivation and justification

Imagine an ideal chain in three-dimensional space, consisting of N "monomers" of size a (the Kuhn length); a shape of the chain corresponds to a N step random walk where each step is represented by a vector whose magnitude is a. Our aim is to obtain an explicit form for the *conditional* probability $P(\mathbf{R}_{mn}|\mathbf{R})$ that the displacement vector from the n-th to the m-th monomer is $\mathbf{R}_{mn} = \mathbf{r}_m - \mathbf{r}_n$, *under the condition* that the end-to-end distance is fixed to $\mathbf{R} = (R_x, R_y, R_z)$. By generalizing the strategy employed in [16] for a ring polymer, we can express this probability as

$$P(\mathbf{R}_{mn}|\mathbf{R}) = \frac{P_{|m-n|}(\mathbf{R}_{mn}) P_{N-|m-n|}(\mathbf{R}_{mn}, \mathbf{R})}{P_N(\mathbf{R})}. \quad (1)$$

Here, $P_N(\mathbf{R})$ is the probability that the end-to-end vector of a unconstrained free polymer is $\mathbf{R}$:

$$P_N(\mathbf{R}) = \prod_{i=x,y,z} \sqrt{\frac{\alpha_N}{\pi}} e^{-\alpha_N R_i^2}, \quad (2)$$

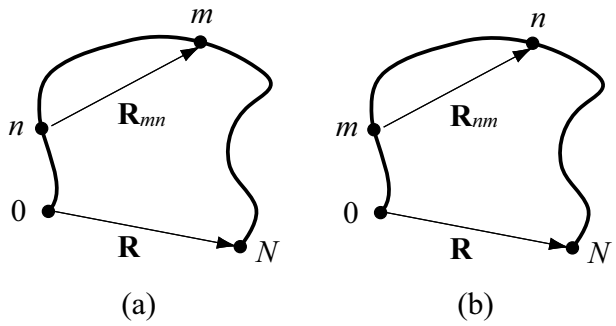

Fig. 1. Configuration of a polymer chain: (a) $n < m$ and (b) $n > m$.

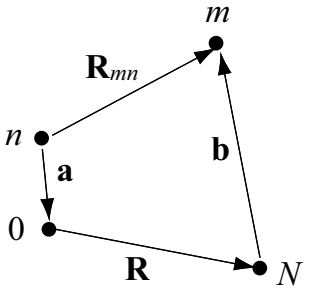

Fig. 2. Definition of vectors correspondig to Figure 1(a).

where $\alpha_N^{-1} = 2Na^2/3$, while $P_{|m-n|}(\mathbf{R}_{mn})$ is the probability for a $|m-n|$ step random walk (with step length a) from the n-th to the m-th monomer with the displacement $\mathbf{R}_{mn}$:

$$P_{|m-n|}(\mathbf{R}_{mn}) = \prod_{i=x,y,z} \sqrt{\frac{\alpha_{|m-n|}}{\pi}} e^{-\alpha_{|m-n|} R_{nm,i}^2}, \qquad (3)$$

where $\alpha_{|m-n|}^{-1} = 2|m-n|a^2/3$.

The meaning of the probability $P_{N-|m-n|}(\mathbf{R}_{mn}, \mathbf{R})$ in equation (1) is slightly different depending on whether n is larger than m or not (see Fig. 1). For $n < m$, $P_{N-|m-n|}(\mathbf{R}_{mn}, \mathbf{R})$ is the probability of the following series of three walks from $\mathbf{r}_n$ to $\mathbf{r}_m$: 1) the first walk from the n-th to the 0th monomer by n *random* steps with step length a, 2) the second walk from the 0th to the N-th monomer by a single *fixed* step vector $\mathbf{R}$, and 3) the third walk from the N-th to the m-th monomer by $N-m$ *random* steps with step length a. The displacement vector for walk 1) is $\mathbf{a}$ while that for walk 3) is $\mathbf{b}$ (see Fig. 2). Since walk 2) is not a random walk ($\mathbf{R}$ is a fixed vector), the successive walk from 1) to 3) is equivalent to making a *single* random walk of $N-m+n$ steps with step length a over the distance $\mathbf{a}+\mathbf{b} = \mathbf{R}_{mn} - \mathbf{R}$.

For $m < n$, $P_{N-|m-n|}(\mathbf{R}_{mn}, \mathbf{R})$ is the probability of the following series of three walks from $\mathbf{r}_m$ to $\mathbf{r}_n$: 1) the first walk from the m-th to the 0th monomer by m steps with step length a, 2) the second walk from the 0th to the N-th monomer by a single step represented by $\mathbf{R}$, and 3) the third walk from the N-th to the n-th monomer by $N-n$ steps with step length a. Similar to the above, this is equivalent to making a random walk of $N-n+m$ steps with step length a over the distance $\mathbf{R}_{nm} - \mathbf{R}$.

Thus, we obtain

$$P_{N-|m-n|}(\mathbf{R}_{mn}, \mathbf{R}) = \qquad (4)$$

$$\prod_{i=x,y,z} \sqrt{\frac{\alpha_{N-|m-n|}}{\pi}} e^{-\alpha_{N-|m-n|}(R_{mn,i} - \zeta R_i)^2}, \qquad (5)$$

where $\zeta = 1$ for $n < m$ and $\zeta = -1$ for $n > m$. Here,

$$\alpha_{N-|m-n|}^{-1} = 2(N-|m-n|)a^2/3. \qquad (6)$$

Substituting equations (2–5) into equation (1), we obtain after some calculation

$$P(\mathbf{R}_{mn}|\mathbf{R}) = \prod_{i=x,y,z} \sqrt{\frac{\alpha_{Nmn}}{\pi}} e^{-\alpha_{Nmn}(R_{mn,i} - R_{mn}^{(0)})^2}, \quad (7)$$

where ζ-dependence in equation (5) disappears. Here,

$$\alpha_{Nmn}^{-1} = 2\mu a^2/3, \qquad (8)$$

$$\mu = \frac{|m-n|(N-|m-n|)}{N}, \qquad (9)$$

$$R_{mn}^{(0)} = \frac{m-n}{N} R_i. \qquad (10)$$

This is one of the important results of our paper. We stress here in advance that equations (11) and (12) below confirm that our probability derived here has the desired property: a chain whose ends are fixed without fluctuation. We remark that, in the limit $\mathbf{R} \to 0$, equation (7) reduces to the known expression for a ring polymer. [14–16].

We can calculate the average of the vector $\mathbf{R}_{mn}$ with the probability $P(\mathbf{R}_{mn}|\mathbf{R})$ (see Eq. (10)):

$$\langle \mathbf{R}_{mn} \rangle = \frac{m-n}{N} \mathbf{R}. \qquad (11)$$

This guarantees that the average of the end-to-end vector takes the expected value, that is, $\langle \mathbf{R}_{N0} \rangle = \mathbf{R}$. In addition, $\langle \mathbf{R}_{nm} \rangle$ deforms "affinely" with $\langle \mathbf{R}_{N0} \rangle (= \mathbf{R})$; $\langle \mathbf{R}_{nm} \rangle$ gets smaller as $|m-n|$ decreases.

The average of $\Delta\mathbf{R}_{mn} \cdot \Delta\mathbf{R}_{mn} = \Delta R_{mn}^2$ with the probability $P(\mathbf{R}_{mn}|\mathbf{R})$, where $\Delta\mathbf{R}_{mn} = \mathbf{R}_{mn} - \mathbf{R}_{mn}^{(0)}$, can be also calculated (see Eqs. (8) and (9)):

$$\langle \Delta R_{mn}^2 \rangle = |m-n|a^2 \left(1 - \frac{|m-n|}{N}\right). \qquad (12)$$

This guarantees that the fluctuation of the end-to-end vector $\langle \Delta R_{N0}^2 \rangle$ is zero: we fix $\mathbf{R}_{N0}$ to $\mathbf{R}$ without fluctuations in our problem. When $|m-n| \neq N$, the fluctuation is not zero: the finite fluctuation $\langle \Delta R_{mn}^2 \rangle$ approaches the value without constraints, $|m-n|a^2$, as $|m-n|$ gets smaller. Here, $\langle \Delta R_{mn}^2 \rangle$ deforms "non-affinely" with $\langle \Delta R_{N0}^2 \rangle (= 0)$.

We can calculate the radius of gyration R_g of this chain by the probability (7):

$$R_{gL}^2 = \frac{Na^2}{36}\left(1 + \frac{3R^2}{Na^2}\right), \qquad R_{gT}^2 = \frac{Na^2}{36},$$

$$R_g^2 = \frac{Na^2}{12}\left(1 + \frac{R^2}{Na^2}\right). \qquad (13)$$

Here, subscripts L and T indicate the components parallel and perpendicular to the fixed vector $\mathbf{R}$. R_g^2 reduces to that for a ring polymer in the limit $\mathbf{R} = 0$ [16] as expected. Note that the transverse component R_{gT}^2 coincides with that of a ring polymer: if a chain whose ends are fixed is projected onto a plane perpendicular to the end-to-end vector $\mathbf{R}$, the chain should look like a ring polymer. This leads to one of the marked differences form the results obtained in the context of networks as mentioned below.

Yamakawa obtained in a general and sophisticated way the one-point probability $P_n(\mathbf{S}_n|\mathbf{R})$ of the displacement vector from the center-of-mass to the n-th monomer being $\mathbf{S}_n$ when the end-to-end vector is fixed to $\mathbf{R}$ (exactly the same constraint as ours). This one-point probability $P_n(\mathbf{S}_n|\mathbf{R})$ can allow us to calculate one-point functions such as the radius of gyration given in equation (13) [18]. Unfortunately, however, this does not make it possible to calculate two-point functions such as the scattering function (*e.g.*, $\langle \mathbf{S}_{nm} \cdot \mathbf{S}_{nm} \rangle$ includes a two-point term proportional to $\langle \mathbf{S}_n \cdot \mathbf{S}_m \rangle$ etc.). This is because we cannot construct a two-point probability $P_{nm}(\mathbf{S}_{nm}|\mathbf{R})$ with $\mathbf{S}_{nm} = \mathbf{S}_n - \mathbf{S}_m$ as a simple multiple of the one-point probabilities, $P_n(\mathbf{S}_n|\mathbf{R})P_m(\mathbf{S}_m|\mathbf{R})$, since the events implied by $P_n(\mathbf{S}_n|\mathbf{R})$ and $P_m(\mathbf{S}_m|\mathbf{R})$ are not independent.

2.2 Comparison with previous results

Benoit *et al.* considered a chain in network deforming affinely with macroscopic deformation where the fluctuation is also affine [7]; we call his model in the following the affine-network (AN) model. Pearson took into account a certain non-affine property in the fluctuation [8] and Warner and Edwards generalized his result [9], whose weak cross-link limit reproduces Pearson's result. We compare below our fixed-end (FE) results with the AN model and with the non-affine–network (NAN) model. The dense cross-link limit of Warner and Edwards model is also mentioned in the context of the scattering function in Section 3.1.

As we see shortly below, the end points of a chain necessarily fluctuate in the AN model and the average of the end-to-end vector is always zero in the NAN model. Both physical assumptions are incompatible with our constraint: the end-to-end vector of a chain is fixed to a non-zero vector without fluctuation. The AN and NAN models are appreciated mainly for a chain in deformed networks. In such a situation, it is known to be reasonable to assume that end points are fluctuating as in the AN model and to incorporate the non-affine nature of a chain as in the NAN model. Accordingly, they have been used to describe a chain in stretched rubbers or gels.

In all the three models, the distribution of $\mathbf{R}_{mn}$ is given by a Gaussian distribution,

$$P\left(\mathbf{R}_{mn}\right) = \prod_{i=x,y,z} \frac{\exp\left(-\frac{(R_{nm,i} - \langle R_{mn,i} \rangle)^2}{2\left\langle \Delta R_{mn,i}^2 \right\rangle} \right)}{\sqrt{2\pi \left\langle \Delta R_{mn,i}^2 \right\rangle}}, \qquad (14)$$

Table 1. The average and the standard deviation of $\mathbf{R}_{mn}$ in the three models.

	$\langle \mathbf{R}_{mn} \rangle$	$\left\langle \Delta R_{mn,i}^2 \right\rangle$
FE	$\frac{m-n}{N}\mathbf{R}$	$\frac{\lvert m-n\rvert a^2}{3}\left(1 - \frac{\lvert m-n\rvert}{N}\right)$
AN	$(m-n)\mathbf{b}$	$\frac{\lvert m-n\rvert a^2}{3}\lambda_i^2$
NAN	$\mathbf{0}$	$\frac{\lvert m-n\rvert a^2}{3} + \frac{(\lambda_i^2-1)(m-n)^2 a^2}{6N}$

Table 2. The average and the standard deviation of the end-to-end vector $\mathbf{R}_{N0}$ in the three models.

	$\langle \mathbf{R}_{N0} \rangle$	$\left\langle \Delta R_{N0,i}^2 \right\rangle$
FE	$\mathbf{R}$	0
AN	$N\mathbf{b}$	$Na^2\lambda_i^2/3$
NAN	$\mathbf{0}$	$Na^2\frac{\lambda_i^2+1}{6}$

where the average and standard deviation of $\mathbf{R}_{mn}$ and those of the end-to-end-vector $\mathbf{R}_{N0}$ are given in Tables 1 and 2, respectively.

Here, $\mathbf{b}$ is a parameter in the AN model (specifying the average end-to-end vector as in Tab. 2) and $\lambda_x = \lambda_y = \lambda_T$ and $\lambda_z = \lambda_L$ are the longitudinal and transverse components of a tensor which describes *the extension of the fluctuation of the end-to-end vector* in the AN and NAN models. More precisely,

$$\frac{\left\langle \Delta R_{N0,i}^2 \right\rangle_\lambda}{\left\langle \Delta R_{N0,i}^2 \right\rangle_0} = \begin{cases} \lambda_i^2, & \text{AN model,} \\ \frac{\lambda_i^2+1}{2}, & \text{NAN model,} \end{cases} \qquad (15)$$

where $\langle \Delta R_{N0,i}^2 \rangle_0$ is the average under no stretch, *i.e.*, $\lambda_T = \lambda_L = 1$. In this case, $\lambda^2 \equiv \lambda_x^2 + \lambda_y^2 + \lambda_z^2 = 3$, which is the minimum of λ^2 under the incompressibility condition: $\lambda_L \lambda_T^2 = 1$.

A similar ratio for the n-to-m vector is given by

$$\frac{\left\langle \Delta R_{mn,i}^2 \right\rangle_\lambda}{\left\langle \Delta R_{mn,i}^2 \right\rangle_0} = \begin{cases} \lambda_i^2, & \text{AN model,} \\ 1 + \frac{(\lambda_i^2-1)\lvert m-n\rvert}{2N}, & \text{NAN model.} \end{cases} \qquad (16)$$

In the AN model, the right-hand side is independent of m and n: this exactly expresses that the fluctuation deforms affinely in the AN model. On the contrary, this is not the case in the NAN model: the NAN model is non-affine.

The average and fluctuation of the end-to-end vector given in Table 2 clarify the difference in constraints between the models: as desired, the end-to-end vector is fixed to $\mathbf{R}$ without fluctuation in our model, while this is not the case with the other models. We can fix the average to $\mathbf{R}$ in the AN model if we set $\mathbf{b} = \mathbf{R}/N$ (as we do in the following for comparison) but the fluctuation cannot be set to zero with a non-trivial physical meaning: if we did set $\lambda = 0$ in the model, the distribution function in equation (14) would become a delta function. In the NAN model the average is zero and cannot be fixed to $\mathbf{R}$;

Table 3. The average of $e^{i\mathbf{q}\cdot\mathbf{R}_{mn}}$ in the three models.

FE	$\exp\left(iq_L R\frac{m-n}{N}\right)\exp\left(-\frac{(qa)^2\lvert m-n\rvert}{6}+\frac{(qa)^2(m-n)^2}{6N}\right)$
AN	$\exp\left(iq_L b(m-n)\right)\exp\left(-\frac{(q_\lambda a)^2\lvert m-n\rvert}{6}\right)$
NAN	$\exp\left(-\frac{(qa)^2\lvert m-n\rvert}{6}-\frac{\left(\left(\lambda_L^2-1\right)q_L^2+\left(\lambda_T^2-1\right)q_T^2\right)a^2(m-n)^2}{12N}\right)$

this model reduces to a chain without constraints when $\lambda_T = \lambda_L = 1$. We clearly see that we cannot describe the correlation of a single chain where the end-to-end vector is fixed to $\mathbf{R}$ without fluctuation by the other models.

3 Scattering function

3.1 Analytical expression

The scattering function is defined by

$$S(\mathbf{q}) = \frac{1}{N^2}\sum_{n,m=1}^{N}\left\langle e^{i\mathbf{q}\cdot\mathbf{R}_{mn}}\right\rangle, \tag{17}$$

where the pair correlation function

$$g(\mathbf{r}) = \frac{1}{N}\sum_{n,m=1}^{N}\left\langle\delta(\mathbf{r}-\mathbf{R}_{mn})\right\rangle, \tag{18}$$

or the average probability of finding a second monomer at a distance $\mathbf{r}$ from a first monomer (the first and the second can be the same), is the direct Fourier transform of $NS(\mathbf{q})$. In principle, this quantity could be calculated from real-space snapshots of a polymer.

In the present model, the average of the quantity $e^{i\mathbf{q}\cdot\mathbf{R}_{mn}}$ with the probability (7) can be cast into the following form:

$$\left\langle e^{i\mathbf{q}\cdot\mathbf{R}_{mn}}\right\rangle = \int \mathrm{d}\mathbf{R}_{mn} P(\mathbf{R}_{mn}|\mathbf{R}) e^{i\mathbf{q}\cdot\mathbf{R}_{mn}} \tag{19}$$

$$= e^{i\mathbf{q}\cdot\mathbf{R}(m-n)/N} e^{-\mathbf{q}\cdot\mathbf{q}\mu a^2/6}. \tag{20}$$

The quantities $\langle e^{i\mathbf{q}\cdot\mathbf{R}_{mn}}\rangle$ in equation (17) of the three models are compared in Table 3. Here, q_λ is the magnitude of a vector $\mathbf{q}$ transformed by a diagonal tensor whose non-zero elements are given by $(\lambda_T, \lambda_T, \lambda_L)$: $\mathbf{q}_\lambda = (\lambda_T q_x, \lambda_T q_y, \lambda_L q_z)$. The dense cross-link limit of the Warner-Edwards model is given by replacing $(m-n)^2$ of the NAN model in Table 3 by a constant independent of m and n.

As seen in Table 3, $\langle e^{i\mathbf{q}\cdot\mathbf{R}_{mn}}\rangle$ of the FE model and of the AN model (with $\mathbf{b} = \mathbf{R}/N$) have the factor $\exp(iq_L R\frac{m-n}{N})$ representing a certain wave character while such a wavy factor is not present in the NAN model (the exponent in the NAN model is always real). This distinction (or considering a Gaussian distribution with non-zero mean) is important: the resulting scattering pattern shows wavy texture in the FE and AN models while the pattern are "monotonous (without such wavy characters)" in the NAN model, as we see below. This distinction has not been made clearly in the literature: equations (29) and (30) of reference [8] and the comment to equation (14) of reference [9] do not care much about the existence of this factor present in the AN model.

The quantity μ in equation (20) is invariant under the interchange of m and n. This guarantees that $S(\mathbf{q})$ is real, and we get

$$S(\mathbf{q}) = 2\,\mathrm{Re}\left[S_0(\mathbf{q})\right], \tag{21}$$

where $(N \gg 1)$,

$$S_0(\mathbf{q}) = \int_0^N \frac{\mathrm{d}m}{N}\int_0^m \frac{\mathrm{d}n}{N}\, e^{i\mathbf{q}\cdot\mathbf{R}(m-n)/N} e^{-\mathbf{q}\cdot\mathbf{q}\mu a^2/6}. \tag{22}$$

If we introduce quantities renormalized by the radius of gyration of a chain without constraints, $R_g^{(0)} = Na^2/6$, as follows:

$$\tilde{R} = R/R_g^{(0)}, \tag{23}$$

$$\tilde{q} = qR_g^{(0)} = \left(q_T^2 + q_L^2\right)^{1/2} R_g^{(0)}, \tag{24}$$

$$\tilde{q}_L = q_L R_g^{(0)}, \tag{25}$$

the scattering function is given by

$$S(\mathbf{q}) = \frac{1}{2\tilde{q}^2}\,\mathrm{Re}\left[1 - e^{i\tilde{q}_L\tilde{R}} + 2Qe^{-(Q^*)^2} S_1(\mathbf{q})\right], \tag{26}$$

where

$$S_1(\mathbf{q}) = \int_{-Q^*}^{Q} \mathrm{d}w e^{w^2} = \frac{\sqrt{\pi}}{2}\left[\mathrm{erfi}(Q) + \mathrm{erfi}\,(Q^*)\right] \tag{27}$$

with

$$Q = \frac{\tilde{q}^2 + i\tilde{q}_L\tilde{R}}{2\tilde{q}}. \tag{28}$$

In the above, the complex error function is defined as

$$\mathrm{erfi}(z) = \frac{2}{\sqrt{\pi}}\int_0^z \mathrm{d}w \exp(w^2), \tag{29}$$

where the complex integral is path-independent due to the regularity of the integrand.

When $\mathbf{R} = 0$, the scattering function for a ring polymer is reproduced [14,15]:

$$S(\mathbf{q}) = \frac{2e^{-\tilde{q}^2/4}\,\mathrm{erfi}\,(\tilde{q}/2)}{\tilde{q}}. \tag{30}$$

3.2 Behavior at small and large scales

$S(\mathbf{q}_T)$ and $S(\mathbf{q}_L)$ at large scales (small q) and small scales (large q) are summarized in Tables 4 and 5, respectively, for comparison ($\mathbf{b} = \mathbf{R}/N$). The expressions at small scales can be obtained by a method similar to derive the asymptotic expansion of the complementary error function [21] while those at large scales by expanding the exponential in terms of $\mathbf{q}$ in equation (17) and evaluating the first and the second moments [22].

Table 4. Scattering function at large scales.

	$S(\mathbf{q}_T)$	$S(\mathbf{q}_L)$
FE	$1-\tilde{q}_T^2/6$	$1-\frac{\tilde{q}_L^2}{6}\left(1+\frac{\tilde{R}^2}{2}\right)$
AN	$1-\frac{1}{3}\left(\lambda_T\tilde{q}_T\right)^2$	$1-\frac{1}{3}\tilde{q}_L^2\left(\lambda_L^2+\frac{\tilde{R}^2}{4}\right)$
NAN	$1-\frac{\tilde{q}_T^2}{12}\left(\lambda_T^2+3\right)$	$1-\frac{\tilde{q}_L^2}{12}\left(\lambda_L^2+3\right)$

Table 5. Scattering function at small scales.

	$S(\mathbf{q}_T)$	$S(\mathbf{q}_L)$
FE	$2/\tilde{q}_T^2$	$2/\tilde{q}_L^2$
AN	$\frac{2}{\left(\lambda_T\tilde{q}_T\right)^2}$	$\frac{2}{\left(\lambda_L\tilde{q}_L\right)^2+\tilde{R}^2}$
NAN	$\frac{2}{\tilde{q}_T^2}\left(1-\frac{\lambda_T^2}{\tilde{q}_T^2}\right)$	$\frac{2}{\tilde{q}_L^2}\left(1-\frac{\lambda_L^2}{\tilde{q}_L^2}\right)$

At large scales, $S(\mathbf{q}_L)$ decays faster than $S(\mathbf{q}_T)$ upon stretch in all the three models (under the incompressibility condition for network models): The more stretch the faster the decay; this suggests the so-called normal butterfly pattern when $S(\mathbf{q})$ is plotted on the (q_T, q_L)-plane: the circular contour shapes for the non-stretched case is compressed along the stretched direction q_L. Physically, this can be understood as follows: the coefficient of q_T^2 or q_L^2 corresponds to the radius of gyration of the chain in that direction [22] so that, when stretched, the coefficient becomes larger in that direction, implying faster decay.

It may be useful to compare the FE model with the AN model at $\lambda_L = \lambda_T = 1$; In this case, the fluctuation of the AN mode is the physically allowed minimum under the incompressible condition of the network (as stated above, we cannot make the AN model fluctuation-less with a non-trivial physical meaning). In the transverse case, $S(\mathbf{q}_T)$ at large scales behaves as that of a ring polymer in the FE model and as that of a linear polymer (without constraints) in the AN model; $S(\mathbf{q}_T)$ in the AN model decays faster than $S(\mathbf{q}_T)$ in the FE model at large scales, which can be again understood as above noting that the coefficient of q_T^2 corresponds to the size of the chain in the transverse direction: a ring polymer is "smaller" than a linear polymer without constraints when the monomer numbers and sizes are the same. At small scales, $S(\mathbf{q}_T)$ of both models behave as that of a linear chain without constraints (see Table 1 with $\lambda_L = \lambda_T = 1$ and $|m-n| \ll N$).

In the longitudinal case, although $S(\mathbf{q}_L)$ at small scales in the FE model is independent of the fixed vector $\mathbf{R}$, it is not the case in the AN model: in the FE model monomers do not feel constraints at small scales while in the AN model they deforms affinely (feeling the constraints at any scales).

3.3 Numerical behavior

We compare the transverse component $S(\mathbf{q}_T)$ as a function of q_T and the longitudinal component $S(\mathbf{q}_L)$ as a function of q_L at $\tilde{R} = 3$ in Figure 3 and at $\tilde{R} = 6$ in Figure 4, in the cases of the FE model. In addition to the above-mentioned faster decay of $S(\mathbf{q}_L)$ in the stretched direction q_L, we see a wavy feature of $S(\mathbf{q}_L)$. This is the result of considering a Gaussian distribution *with a non-zero mean*, which leads to the factor $\exp(iq_L R\frac{m-n}{N})$ in Table 3 or the factor $i\tilde{q}_L\tilde{R}$ in equations (26) and (27): the wavelength of the wave is of the order of $2\pi/R$.

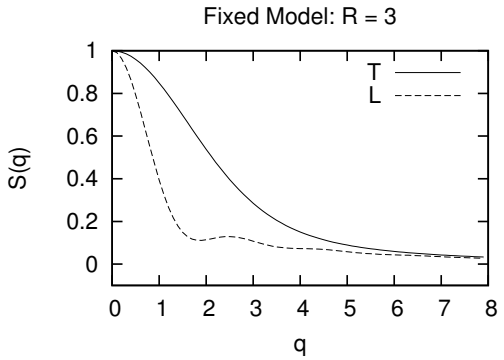

Fig. 3. The scattering function $S(\mathbf{q})$ of the FE model as a function of $q = q_T$ (solid curve) or $q = q_L$ (dashed curve) when the distance between the ends is fixed at $R = 3$, where q and R are normalized by the radius of gyration of a linear chain $R_g^{(0)}$ (this normalization is always employed in Figs. 4-12 below). The solid and dashed curves correspond to the transverse and longitudinal component, respectively.

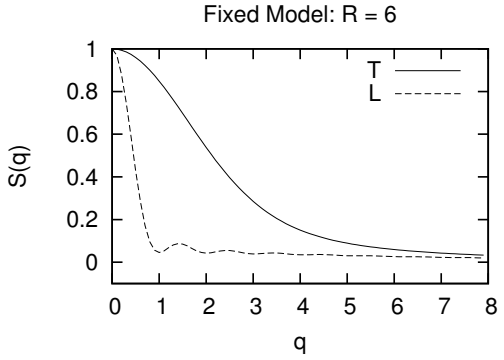

Fig. 4. The scattering function $S(\mathbf{q})$ of the FE model as a function of $q = q_T$ (solid curve) or $q = q_L$ (dashed curve) at $R = 6$.

The three-dimensional and the contour plots of $S(\mathbf{q})$ on the (q_T, q_L)-plane are shown in Figures 5 and 6, respectively. We notice a normal butterfly pattern in the sense that the contour shapes tend to be compressed in the stretched direction q_L. There are a number of differences from the butterfly pattern of gels [12,13]: 1) a two-lobe feature in the gel butterfly pattern is less visible (this feature comes from the singularity of $S(\mathbf{q})$ in gel models at $\mathbf{q} = 0$: there is a gap between $\lim_{q_T\to 0} S(q_T)$ and $\lim_{q_L\to 0} S(q_L)$). 2) A wavy texture at intermediate $\mathbf{q}$ is visible in the FE model, which is not present in the conventional butterfly models. Note also that we consider here rather strongly stretched cases ($\tilde{R} > 1$). When weakly stretched, contour shapes are simple ellipses similar to those in Figure 12 below.

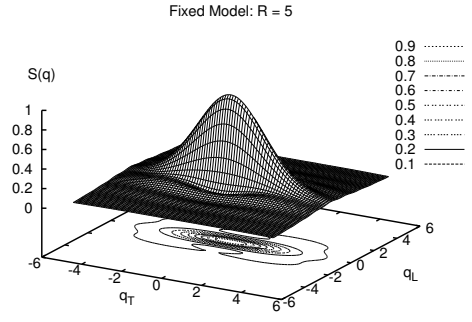

Fig. 5. The scattering function $S(\mathbf{q})$ of the FE model on the (q_T, q_L)-plane at $R = 5$.

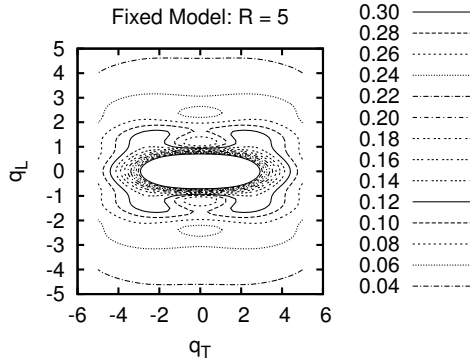

Fig. 6. The contour plot of $S(\mathbf{q})$ of the FE model on the (q_T, q_L)-plane at $R = 5$. The highest contour shown here is limited to $S(\mathbf{q}) = 0.3$.

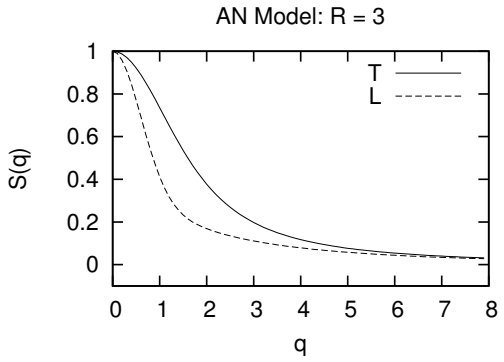

Fig. 7. The scattering function $S(\mathbf{q})$ of the AN model with the minimum fluctuation ($\lambda_T = \lambda_L = 1$) as a function of $q = q_T$ (solid curve) or $q = q_L$ (dashed curve) at $R = 3$.

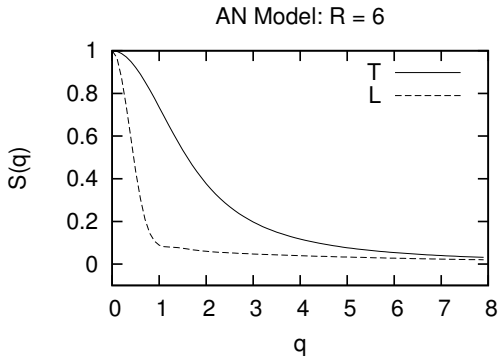

Fig. 8. The scattering function $S(\mathbf{q})$ of the AN model with the minimum fluctuation ($\lambda_T = \lambda_L = 1$) as a function of $q = q_T$ (solid curve) or $q = q_L$ (dashed curve) at $R = 6$.

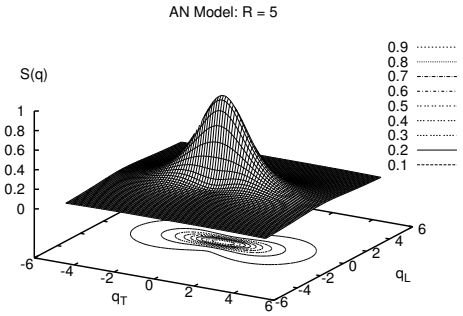

Fig. 9. The scattering function $S(\mathbf{q})$ of the AN model with the minimum fluctuation on the (q_T, q_L)-plane at $R = 5$.

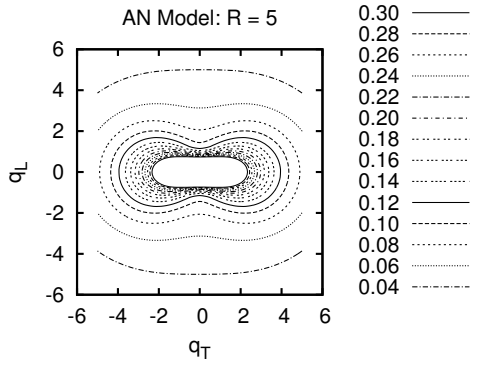

Fig. 10. The contour plot of $S(\mathbf{q})$ of the AN model with the minimum fluctuation on the (q_T, q_L)-plane at $R = 5$. The highest contour shown here is again limited to $S(\mathbf{q}) = 0.3$.

In Figures 7 to 10 we show the plots of the AN model with the minimum fluctuation ($\lambda_L = \lambda_T = 1$) corresponding to those of the FE model in Figures 3 to 6, respectively. We see that the wavy texture is less significant in the AN model than in the FE model. Because of this, the two-lobe feature on the contour plot in the AN model (Fig. 10) is more visible than in the FE model (although $S(\mathbf{q})$ at $\mathbf{q} = 0$ is not singular in these two models).

In Figures 11 and 12 we show the three-dimensional and the contour plots of $S(\mathbf{q})$ of the NAN model on the (q_T, q_L)-plane. We set $\lambda_L = 5$ and $\lambda_T = 1/\sqrt{\lambda_L}$ (incompressible network). Although we cannot quantitatively compare these plots with those of the FE and AN models because the average of the end-to-end vector of the NAN model is zero, we remark that the two-lobe feature is completely absent in the NAN model.

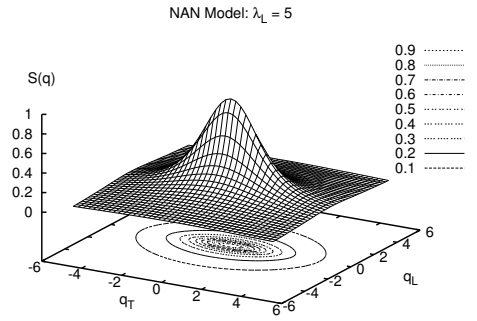

Fig. 11. The scattering function $S(\mathbf{q})$ of the NAN model with $\lambda_L = 5$ and $\lambda_T = 1/\sqrt{\lambda_L}$ on the (q_T, q_L)-plane at $R = 5$.

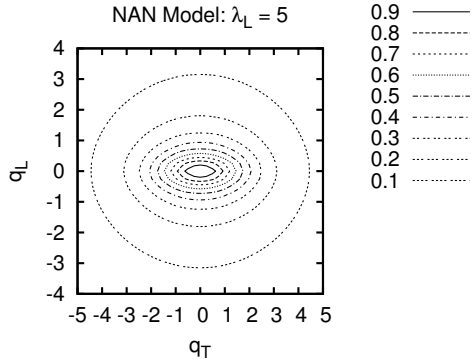

Fig. 12. The contour plot of $S(\mathbf{q})$ of the NAN model with $\lambda_L = 5$ and $\lambda_T = 1/\sqrt{\lambda_L}$ on the (q_T, q_L)-plane at $R = 5$.

4 Conclusion

We derived a two-point probability distribution $P(\mathbf{R}_{mn}|\mathbf{R})$ in equation (7) for a chain whose ends are fixed without fluctuation. We find that the average of $\mathbf{R}_{mn}$ behaves "affinely" as in equation (11) while the standard deviation behaves "non-affinely" as in equation (12), which are consistent with the original constraint. The resulting scattering function shows a kind of normal butterfly pattern: the contour shape on the (q_T, q_L)-plane is compressed in the longitudinal direction. Notably, the pattern is textured with a wavy character.

We compared our results with some previous models and clarified the meaning of the previous models in terms of the average and the standard deviation of $\mathbf{R}_{mn}$ of a Gaussian model as in Tables 1 and 2: the AN model necessarily has a finite magnitude of fluctuation at both ends although the average end-to-end distance is fixed, while the average end-to-end distance is zero and both ends are fluctuating in the NAN model. We cannot describe a chain whose ends are fixed without fluctuation by the AN and NAN models.

We comment on a possible connection of these models with the recently obtained scattering function of stretched slip-ring gels [20]. When such a gel is stretched, the inhomogeneity in the cross-link density, which is the origin of the abnormal butterfly pattern (the contour shape is elongated in the longitudinal direction), becomes weak and each chain looks as if its average end-to-end distance was fixed but with a weak fluctuation: from our interpretation, the latter situation would be described (especially when the chain is in θ-solvent or in melt) by the AN model, or, in some cases, by the FE model.

Recently, Sommer and Saalwächer studied segmental order in end-linked polymer networks [23]. In their study, they consider a chain polymer with its ends fixed and under this constraint they calculated numerically a tensor order parameter. It is shown that this quantity measurable via NMR can markedly distinguish swollen chains and chains in gel from ideal chains. In this context, it would be worthwhile studying the tensor order parameter by using the analytical distribution for the end-fixed ideal chain obtained in this work. This point will be examined in the near future.

K.O. thanks Katsumi Hagita and Tetsuo Deguchi for getting their attention to reference [18] and references [14,15], respectively. This work is supported by research grants KAKENHI (MEXT, Japan).

References

1. M. Nierlich, C. Williams, F. Boué, J.P. Cotton, M. Daoud, M. Farnoux, G. Jannink, C. Picot, J. Appl. Cryst. **11**, 504 (1978).
2. M. Shibayama, H. Kurokawa, S. Nomura, S. Roy, R.S. Stein, W.-L. Wu, Macromolecules **23**, 1438 (1990).
3. E. Moses, T. Kume, T. Hashimoto, Phys. Rev. Lett. **72**, 2037 (1994).
4. H. Benoit, D. Decker, R. Duplessix, C. Picot, P. Rempp, J.P. Cotton, B. Farnoux, G. Jannink, R. Ober, J. Polym. Sci., Polym. Phys. Ed. **14**, 2119 (1976).
5. E. Mendes jr., P. Lindner, M. Buzier, F. Boué, J. Bastide, Phys. Rev. Lett. **66**, 1595 (1991).
6. Y. Arai, R. Yasuda, K. Akashi, Y. Harada, H. Miyata, K. Kinosita jr., H. Itoh, Nature **399**, 446 (1999).
7. H. Benoit, B. Duplessix, R. Ober, M. Daoud, J.P. Cotton, B. Farnoux, G. Jannink, Macromolecules **8**, 451 (1975).
8. D.J. Pearson, Macromolecules **10**, 696 (1977).
9. M. Warner, S.F. Edwards, J. Phys. A: Math. Gen. **11**, 1649 (1978); R.T. Deam, S.F. Edwards, Philos. Trans. R. Soc. London, Ser. A **280**, 317 (1976).
10. P. Pincus, Macromolecules **9**, 386 (1976).
11. P.G. de Gennes, *Scaling Concepts in Polymer Physics* (Cornell University Press, Ithaca, 1979).
12. J. Bastide, L. Leibler, J. Prost, Macromolecules **23**, 1821 (1990).
13. A. Onuki, J. Phys. II **2**, 45 (1992).
14. E.F. Casassa, J. Polym. Sci. A **3**, 605 (1965).
15. W. Burchard, M. Schmidt, Polymer **21**, 745 (1980).
16. A.Y. Grosberg, A.R. Khokhlov, *Statistical Physics of Macromolecules* (AIP Press, New York, 1994).
17. For the recent developement, see M.K. Shimamura, K. Kamata, A. Yao, T. Deguchi, Phys. Rev. E **72**, 041804 (2005) and references therein.
18. H. Yamakawa, *Modern Theory of Polymer Solutions* (Harper & Row, New York, 1971).

19. M. Rubinstein, R.H. Colby, *Polymer Physics* (Oxford University Press, New York, 2003).
20. T. Karino, Y. Okumura, C. Zhao, T. Kataoka, K. Ito, M. Shibayama, Macromolecules **38**, 6161 (2005).
21. See for example, Chapt. 11 of M.L. Boas, *Mathematical Methods in the Physical Sciences*, 2nd ed. (John Wiley & Sons, Inc., New York, 1983).
22. See for example, Chapt. 2 of M. Doi, S.F. Edwards, *The Theory of Polymer Dynamics* (Oxford University Press Inc., New York, 1986).
23. J.-U. Sommer, K. Saalwächer, Eur. Phys. J. E **18**, 167 (2005).